OPEN ACCESS

Saudi Journal of Engineering and Technology
Abbreviated Key Title: Saudi J Eng Technol
ISSN 2415-6272 (Print) |ISSN 2415-6264 (Online)
Scholars Middle East Publishers, Dubai, United Arab Emirates
Journal homepage: https://saudijournals.com

Review Article

# Exploring the Dynamics of Viscous Dissipative Fluid past a Super-hydrophobic Microchannel in the Coexistence of Mixed Convection and Porous Medium

Godwin Ojemeri[1*], I. O. Onwubuya[2]

[1]Department of Mathematics, College of Sciences, Federal University of Agriculture, P. M. B. 28, Zuru, Kebbi State, Nigeria
[2]Department of Mathematics, Faculty of Sciences, Air Force Institute of Technology, P. M. B. 2104, Kaduna State, Nigeria

**DOI:** 10.36348/sjet.2023.v08i04.001 | **Received:** 15.03.2023 | **Accepted:** 26.04.2023 | **Published:** 30.04.2023

***Corresponding author:** Godwin Ojemeri
Department of Mathematics, College of Sciences, Federal University of Agriculture, P. M. B. 28, Zuru, Kebbi State, Nigeria

## Abstract

This article investigates the theoretical treatment of mixed convection heat enhancement flow for an electrically-conducting and viscous dissipative fluid traveling vertically through a thermodynamic system where the parallel plates are constantly heated in a slit micro-channel due to mixed convection with porous material. One surface had super-hydrophobic slip and a temperature jump, whereas the other did not. The perturbation technique (semi-analytical method) was employed to solve the nonlinear and coupled leading equations. The results were carefully scrutinized, and the effects of the relevant controlling parameters are shown using different plots. It is concluded from this analysis that the fluid temperature and velocity was found to increase as the viscous dissipation term is increased. Similarly, the function of Darcy porous number is to significantly strengthen the fluid velocity, and these effects are stronger at the heated super-hydrophobic surface, whereas mounting level of magnetic field is seen to drastically weaken the fluid motion in the microchannel. Setting Br and A to zero respectively, $\frac{Gr}{Re} = 1$, and Da to 1000, so that the term $\frac{1}{Da}$ becomes insignificant, Jha and Gwandu (2017)'s work is retrieved, verifying the accuracy of the current analysis. Further, the outcomes of this research can have possible applications in the lubrication industry and biomedical sciences and has proved very useful to designers in increasing the performance of mechanical systems when viscous dissipation is involved, as well as heat transfer in micro-channels, as it is in combustion.

**Keywords:** Super-hydrophobic slip, Temperature jump, Viscous dissipation, Mixed convection, Porous medium, Micro-channel.



## 1. INTRODUCTION

The rapid growth of technology in response to people's desires for smaller machines and lighter devices directs the scientific community, engineers, and innovators' attention to exploration, simulation, and theoretical investigations in mini-technology, then micro-technology, and finally nano-technology. This is what prompted fluid mechanics experts to go from researching flows in macro-channels to researching flows in mini-channels, micro-channels, and nano-channels. Micro-channel fluid and thermal transport flows have grown tremendously in recent times as a result of their wide spectrum of interesting applications in material processing activities and fabrication; micro energy pipes; space technology; micro-channel internal heat generation; micro-jet boundary layer cooling; large power density transistors in high-performance computing; and other devices. Since most of these designs involve internal micro-channel flows, comprehending the flow characteristics has become extremely crucial for proper and appropriate simulation projections and conceptualization [1, 2]. Numerous studies have been published on the role of the flow regime on micro-geometry in a number of physical situations. In light of the foregoing, Hamza *et al.*, [3] recently published a theoretical study on the impact of Arrhenius-controlled heat transfer flow influenced by an induced magnetic field in a microchannel. Ojemeri and Hamza [4] investigated the consequences of Arrhenius kinetically driven heat source/sink fluid in a microchannel using the homotopy perturbation technique. Jha and Malgwi [5] analyzed the effects of

Hall current and ion-slip on hydro-magnetic heat transfer flow in a vertical micro-channel with an applied magnetic field. Jha and Aina [6] comprehensively addressed natural convection driven hydro-magnetically in a vertical micro-channel made of two electrically non-conducting infinite vertical parallel plates. In another work, Jha *et al.*, [7] deliberated on the consequences of Hall currents on hydro-magnetic natural convection in a vertical micro-channel. References that beamed more searchlight on this field of interest include [8-12], to name a few.

Magneto-hydrodynamics (MHD) research has evolved in prominence in recent decades owing to the concept's benefits in a range of MHD applications, namely magneto-hydrodynamic (MHD) generators, optical grafting, metal casting, crystal growth, and magneto-hydrodynamic injectors. Several nuclear power facilities already use chemical energy technology, which incorporates the use of MHD pumps to move electrically conductive fluids. In addition to these applications, when the fluid is electrically conducting, an applied magnetic field can considerably increase free convection flow [13]. Various research has been conducted on hydro-magnetic convective flow under a spectrum of environmental situations. To this end, Ojemeri *et al.*, [14] investigated the MHD-free flow of a Casson fluid that is electrically conductive, influenced by thermal radiation effect in a vertical porous channel. Hamza *et al.*, [15] discussed the implications of MHD on natural convective slip flow of an exothermic fluid due to Newtonian heating. Taid and Ahmed [16] used the perturbation approach to probe the impacts of the soret effect, heat dissipation, and chemical reaction on steady two-dimensional hydro-magnetic natural convection across an inclined porous plate coated with porous media. Osman *et al.* [17] searched the function of magneto-hydrodynamics on free convection over an infinite inclined plate using the Laplace transformation technique. Siva *et al.*, [18] presented a precise response to the MHD action on a heat enhancement study of electroosmotic flow in a rotating microfluidic channel. Heat and mass transportation were probed for viscoelastic MHD boundary layer flow past a vertical flat plate by Choudhary [19]. The actions of an inclined magnetic field on the time-dependent natural convection flow of a dusty viscous fluid within two infinite flat plates packed with a porous material was examined by Sandeep and Sugunamma [20]. When Joseph *et al.*, [21] discussed unsteady MHD poiseuille flow across two infinitely parallel porous plates in an inclined magnetic field, they also considered the impacts of heat and mass transport. They discovered that as the Hartman number Ha grows, the velocity drops. Velocity rises due to the thermal Grashof number Gr and the solutal Grashof number Gc influences. A boost in the Prandtl number, Pr, leads to a decaying in the fluid temperature. As the chemical parameter Kc and the Schmidt number Sc rise, so does the concentration of a species. Geethan *et al.*, [22] scrutinized the joint consequences of thermal radiation, chemical reaction, and Soret on hydro-magnetic free convection slip flow along an inclined plate with constant temperature affected by heat source. A computational analysis of the Hall current and thermal radiation effects of MHD natural convective mass and energy transfer radiating fluid flow in the Soret effect and heat generation was accounted for by Sivaiah and Reddy [23]. Scientists, technologists, and engineers are paying much attention to the evaluation of the result of the new combination using hydro-magnetic natural convection flow in a super-hydrophobic (SHO) micro-channel. Oil and gas companies, semiconductor manufacturing facilities, and companies that assemble small equipment SHO surfaces have the ability to reduce drag in a flow because of the enormous slip obtained from liquid/solid interfaces, making it a particularly relevant parameter to gauge the extent of drag reduction depending on the slip length. In view of these considerations, a theoretical investigation of MHD natural convection in a vertical slit micro-channel having super-hydrophobic slip effect and temperature jump was conducted by Jha and Gwandu[1]. Their research showed that the greatest upward velocity obtained by heating the super-hydrophobic wall is less than that attained by heating the no-slip surface whenever there is a temperature leap and no super-hydrophobic slip, or both. The maximum velocities are equivalent when neither is present. Later, Jha and Gwandu [24] investigated free convection flow of an electrically conducting fluid in a vertical slit micro-channel affected by super-hydrophobic slip and temperature jump effects using the non-linear Boussinesq approximation methods. Raising the temperature jump coefficient, according to the computational results, contributes to a decrease in temperature when the super-hydrophobic surface is heated and increases the temperature when the no-slip surface is heated. Jha and Gwandu [25] built on their previous work Jha and Gwandu [1] by proposing an analytical investigation of free convection airflow across porous plates heated alternately, one channel with no slip and the other super-hydrophobic. Ramanuja *et al.*, [26] explored free convection flow in an isothermally heated channel with super-hydrophobic slip on one surface and a temperature rise, but no slip on the opposite side. Hatte and Pitchumani [27] used a fractional rough surface characterization to thoroughly and explicitly describe the impact of heat transfer flow inside a cylinder with non-wetting surfaces. The approach examines the dynamic stability of the air/fluid interaction in the asperities of air-infused super-hydrophobic surfaces. Their findings show that, contrary to prevalent belief, super-hydrophobicity, defined by the largest contact angles, does not always result in peak convective heat transfer behavior and that, under specific fluid flow conditions, hydrophobic surfaces can provide excellent thermal performance.

The impacts of mixed convection, viscous dissipation and Darcy permeability on micro-channels with super-hydrophobic (SHO) surfaces have not been examined in a single work in any of the above-mentioned literature, which prompted the interest for this research. Thus, motivated by the above knowledge gap, the focus of this paper is to theoretically investigate the impact of MHD free convection flow of viscous dissipative fluid in a vertical parallel plates that is constantly heated in a slit micro-channel having a super-hydrophobic surface filled with porous media. To the best of the authors' knowledge, this research has not been documented in any earlier literature, resulting in the study's novelty. A semi-analytical approach (perturbation method) was employed to solve the dimensionless nonlinear and coupled governing equations. The behaviors of controlling parameters on the temperature, velocity, heat transfer rate and sheer stress was computed and discussed with the help of illustrative graphs. The results of this study could be used in many different ways, such as in micro-devices made with micro-fabrication techniques, cooling of nuclear reactors, cooling of electric appliances, in micro-electro-mechanical systems (MEMS), in the lubrication industry, in biomedical sciences, in the processing and extraction industries, and so on.

**2. Mathematical Formulation of the Problem**

Imagine an electrically conducting fluid travelling gradually upward within vertical parallel plates micro-channel heated alternatively by wall constant temperature. Due to a particular micro-engineering treatment, one of the surfaces is exceedingly difficult to wet (super-hydrophobic). The opposite wall (no-slip surface) was unaltered. As shown in Fig. 1, the super-hydrophobic wall is kept at $y_0 = 0$, while the no-slip surface is kept at $y_0 = L$. Since the ultimate focus is on the super-hydrophilicity of a surface rather than the flow behavior, various temperature jump and slip conditions were applied to the plates. Following Jha and Gwandu [1], the leading equations for the current problem are as follows, employing the Boussinesq buoyancy approximation with boundary conditions and assuming that the fluid is viscous dissipative, and in the coexistence of mixed convection and porous medium.

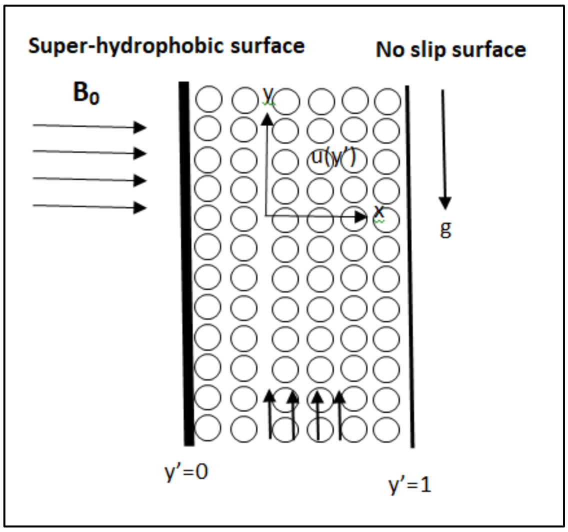


**Figure 1: Schematic of the fluid flow in a slit microchannel with a porous configuration**

$$\frac{d^2U}{dy^2} + \frac{Gr}{Re}\theta - \left(M^2 + \frac{1}{Da}\right)U = A \qquad (1)$$

$$\frac{d^2\theta}{dy^2} + Br\left(\frac{du}{dy}\right)^2 = 0 \qquad (2)$$

The boundary conditions in dimensionless forms are:

$$\theta(0) = 1 + \gamma\frac{d\theta}{dy}, u(0) = \lambda\frac{du}{dy} \qquad (3)$$
$$\theta(1) = 0, u(1) = 0$$

Where $\frac{Gr}{Re} = Gr$ is the mixed convection, M is the magnetic field intensity, Da is the permeability of the porous medium, $A = \frac{dP}{dX}$ is the pressure gradient, Br = EcPr is the Brinkman number, $\gamma$ is the temperature jump coefficient and $\lambda$ is the velocity slip condition.

The dimensional quantities used in deriving equations 1-3 are as follows:

$$u = \frac{u'}{U}, \quad y = \frac{y'}{h}, \quad T = \frac{T' - T_0}{T_w - T_0}, \quad x = \frac{x'v}{Uh^2}, \quad M^2 = \frac{\sigma\beta_0^2 h^2}{\rho v},$$

$$Da = \frac{\kappa}{h^2}, Br = \frac{hH}{k}, Gr = \frac{g\beta(T_1 - T_0)x^3}{v^2}, \quad \mathrm{Re} = \frac{u_0 x}{v},$$

$$A = -\frac{\partial P}{\partial x}, \quad (Y, \gamma, \lambda) = (Y', \gamma', \lambda')/h$$

All the constants used are declared in the nomenclature

## 3. METHOD OF SOLUTION

The velocity and energy equations can be reduced to the set of ordinary differential equations, which are solved semi-analytically by perturbation method.

we assume
$$\left.\begin{aligned}\theta &= \theta_o + B_r\theta_1 \\ U &= U_o + B_r U_1\end{aligned}\right\} \qquad (4)$$

substituting eqn (4) into eqns (1-3) and taking the coefficient of $B_r^o$ and $B_r$, we have

$$B_r^o: \frac{d^2U_o}{dy^2} + \frac{Gr}{Re}\theta_o - (M^2 + \frac{1}{Da})U_o = A \quad (5)$$

$$B_r: \frac{d^2U_1}{dy^2} + \frac{Gr}{Re}\theta_1 - (M^2 + \frac{1}{Da})U_o = 0 \quad (6)$$

$$B_r^o: \frac{d^2\theta_o}{dy^2} = 0 \quad (7)$$

$$B_r: \frac{d^2\theta_1}{dy^2} + (\frac{dU_o}{dy})^2 = 0 \quad (8)$$

The boundary conditions at the both walls now becomes

$$\left.\begin{aligned} B_r: \theta_1 &= \gamma\frac{d\theta_1}{dy} \\ U_1 &= \lambda\frac{dU_1}{dy} \end{aligned}\right\} at\ y = 0 \quad (9)$$

$$\left.\begin{aligned} &\left.\begin{aligned} U_o &= \lambda\frac{dU_o}{dy} \\ U_1 &= \lambda\frac{dU_1}{dy} \end{aligned}\right\} at\ y = 0 \\ &\left.\begin{aligned} U_o &= 0 \\ U_1 &= 0 \end{aligned}\right\} at\ y = 1 \end{aligned}\right\} \quad (10)$$

$$\left.\begin{aligned} &\left.\begin{aligned} \theta_o &= 1 + \gamma\frac{d\theta_o}{dy} \\ \theta_1 &= \gamma\frac{d\theta_1}{dy} \end{aligned}\right\} at\ y = 0 \\ &\left.\begin{aligned} \theta_o &= 0 \\ \theta_1 &= 0 \end{aligned}\right\} at\ y = 1 \end{aligned}\right\} \quad (11)$$

Solution for temperature distribution is derived as follows:

$$\theta_o = V_1y + V_2 \quad (12)$$

$$\theta_1 = -\frac{a_1}{4m^2}e^{2my} - \frac{a_2}{m^2}e^{my} - \frac{a_3}{m^2}e^{-my} - \frac{a_4}{4m^2}e^{-2my} - a_5\frac{y^2}{2} + V_7y + V_8 \quad (13)$$

Solution for velocity distribution is obtained as follows:

$$U_0 = V_3e^{my} + V_4e^{-my} + V_5y + V_6 \quad (14)$$

$$U_1 = F_1e^{my} + F_2e^{-my} + F_3e^{2my} + F_4ye^{my} + F_5ye^{-my} + F_6e^{-2my} + F_7y^2 + F_8y + F_9 \quad (15)$$

Since $\theta = \theta_0 + B_r\theta_1$ (16)

Then

$$\theta = V_1y + V_2 + B_r\left[-\frac{a_1}{4m^2}e^{2my} - \frac{a_2}{m^2}e^{my} - \frac{a_3}{m^2}e^{-my} - \frac{a_4}{4m^2}e^{-2my} - a_5\frac{y^2}{2} + V_7y + V_8\right] \quad (17)$$

also, since $U = U_0 + B_rU_1$ (18)

then

$$U = V_3e^{my} + V_4e^{-my} + V_5y + V_6 + B_r[F_1e^{my} + F_2e^{-my} + F_3e^{2my} + F_4ye^{my} + F_5ye^{-my} + F_6e^{-2my} + F_7y^2 + F_8y + F_9] \quad (19)$$

The heat transfer rate and frictional force at both plates are derived as follows:

$$\frac{d\theta}{dy}\Big|_{y=0} = V_1 + B_r\left[-\frac{a_1}{2m} - \frac{a_2}{m} + \frac{a_3}{m} + \frac{a_4}{2m} + V_7\right] \quad (20)$$

$$\frac{d\theta}{dy}\Big|_{y=1} = V_1 + B_r\left[-\frac{a_1}{2m}e^{2m} - \frac{a_2}{m}e^{m} + \frac{a_3}{m}e^{-m} + \frac{a_4}{2m}e^{-2m} - a_5 + V_7\right] \quad (21)$$

$$\frac{dU}{dy}\Big|_{y=0} = V_3m - V_4m + V_5 + B_r[F_1m - F_2m + 2F_3m + F_4 + F_5 - 2F_6m + F_8] \quad (22)$$

$$\frac{dU}{dy}\Big|_{y=1} = V_3me^m - V_4me^{-m} + V_5 + B_r[F_1me^m - F_2me^{-m} + 2F_3me^{2m} + F_4me^m + F_4e^m$$
$$+F_5me^{-m} + F_5e^{-m} - 2F_6me^{-2m} + 2F_7 + F_8] \quad (23)$$

All the constants used are defined in the appendix section

## 4. RESULTS AND DISCUSSION

This paper examined the consequences of MHD mixed convection and viscous dissipation on the flow of an incompressible electrically-conducting fluid traveling vertically inside an isothermally heated parallel plate micro-channel saturated with porous material, with one surface having super-hydrophobic slip and temperature jump and the other having no slip. The perturbation series approach (semi-analytical method) is used to evaluate the steady state governing equations. Several graphs were drawn to showcase the influences of various settings on the flow configuration and energy profile. The default values chosen for this research are (λ = γ = 1, M=0.5, Br=0.001, Gre=10, A=1, Da=0.1), except otherwise stated, as it relates to real life situation

Figures 2 and 3 show the impact of the Brinkman number (Br) on dimensionless thermal and momentum distributions for fixed values of (λ = γ = 1). It is obvious from these figures that the thermal and movement of the fluid increase dramatically as the local Brinkman number (Br) increases. Higher Brickman values indicate stronger convective heating at the lower channel surface, resulting in a better temperature and velocity at the lower plate. Makinde and Aziz [28] opined that uplifting the local Brinkman numbers makes the convective heating at the lower channel wall stronger. This leads to higher surface temperatures and lets the thermal effect go deeper into the still fluid.

Figure 4 depicts the action of the Darcy porosity parameter on the velocity gradient. It is perceived from this figure that the velocity fluid accelerates as the porosity parameter is increased. We observe that, with the growth in permeability of the porous medium, the drag force weakens; because of this, velocity gradient of the fluid blows up. Moreover, this makes sense because when a lot of fluid is moved, more viscous energy is made. This causes the fluid boundary wall and thickness to grow, which speeds up the movement of the fluid.

Figure 5 plots the behavior of velocity for the deviations of mixed convection parameter. It is observed that uplifting the level of the mixed convection parameter, the fluid velocity is drastically enhanced in the microchannel.

With the help of Fig. 6, we comprehend how velocity distribution behave against displacement y, and the outcome is consistent to what has been discovered in previously published works by other authors. This demonstrates that as particles move out from the super-hydrophobic side, their velocity increases for a short time before petering as it approaching the center. However, if both surfaces are not super-hydrophobic, the velocity does not rise significantly and does not fall until near the channel's center.

Figure 7 showcases the function of MHD on the velocity gradient. The pattern demonstrates a decrease in the fluid flow (particularly the peak velocity) as the magnetic field intensity increases (when both λ and γ are each equal to unity). This is so attributable to the Lorentz force, which appears when aa magnetic field imposes to an electrically conducting fluid and a drag force is created. Due to this force, fluid movement dwindle near the plate; all other forces including Lorentz force peters out as a result when the fluid comes to rest.

Figures 8 and 9 show the implication of the Brinkman number (Br) on the rate of heat transfer coefficient and wall shear stress. Heat transfer rate upsurges for growing values of Brinkman number in both walls. The effect of large Br is seen to strengthen the frictional force (at y = 0) as shown in Fig. 8a, whereas a reverse trend is obtained (at y = 1) as depicted in figure 8b.

Figure 10 displays the action of a magnetic field on skin friction. It's clear that MHD has the same effect on sheer stress on both plates, but this impact is stronger at the plate where y = 0.

The Darcy porous effect on frictional force at both plates is plotted in Figure 11. It can be seen that identical ascending tendencies are recorded on both walls.

The influence of mixed convection parameter on the sheer stress is demonstrated in figure 12. It is evident that at the both microchannel walls, similar downward trend is noticed for increasing values of Gre.

## 5. VALIDATION

The work of Jha and Gwandu [1] is retrieved by setting Br and A to zero, Gre=1 and Da = 1000, thereby confirming an excellent agreement between this present research and their work. Table 1 describes the numerical computations of the comparison between the work of Jha and Gwandu [1] and the current investigation.

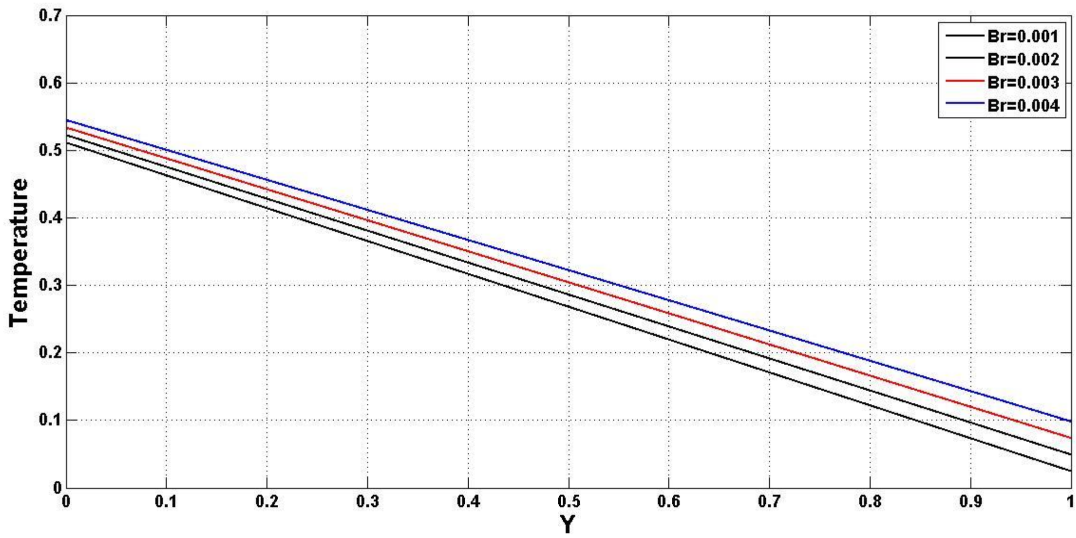


**Figure 2: Deviation of temperature for Br for constants values of (λ = γ = 1, M=0.5, Da=0.1)**

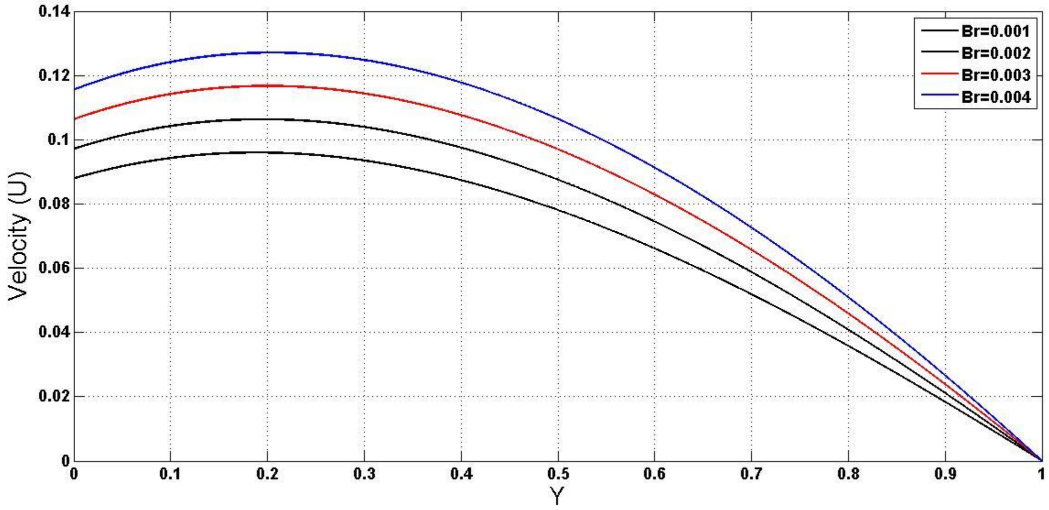


**Figure 3: Deviation of velocity for Br for constants values of (λ = γ = 1, M=0.5, Da=0.1)**

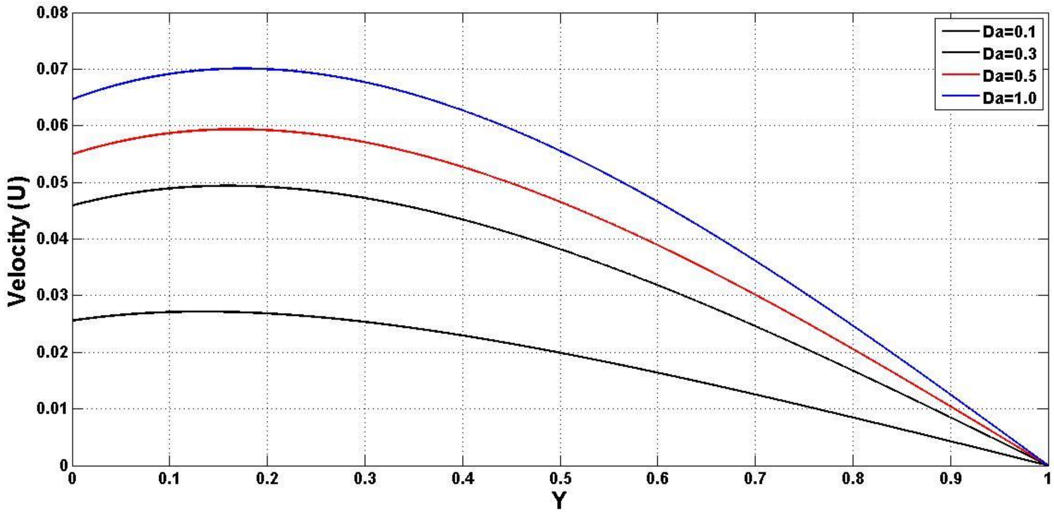


**Figure 4: Deviation of velocity for Da for constants values of (λ = γ = 1, M=0.5)**

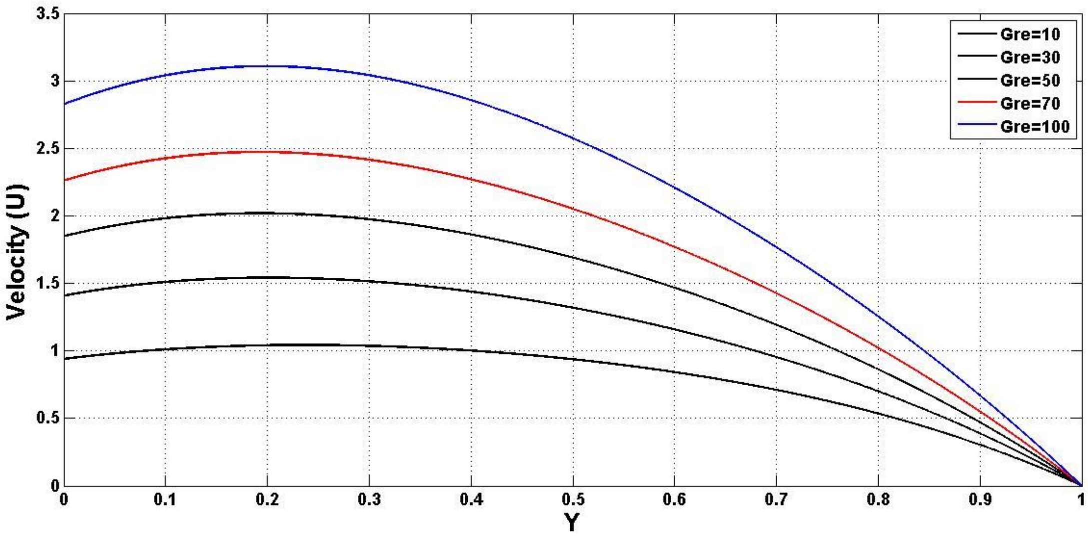


**Figure 5: Deviation of velocity for Gre for constants values of (λ = γ = 1, M=0.5)**

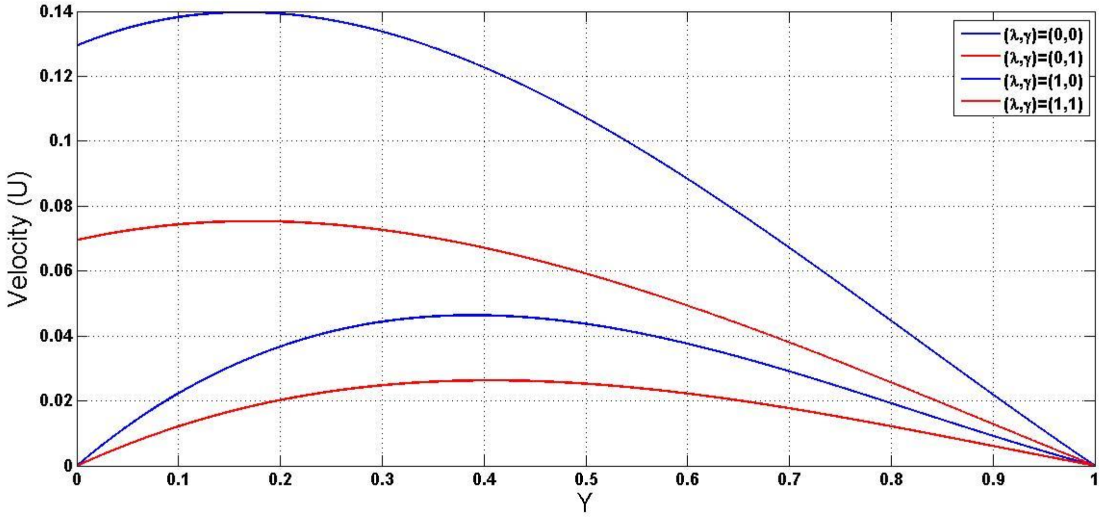


**Figure 6: Deviation of velocity for the displacement y for constants values of (M=0.5, Br=0.001, Da=0.1)**

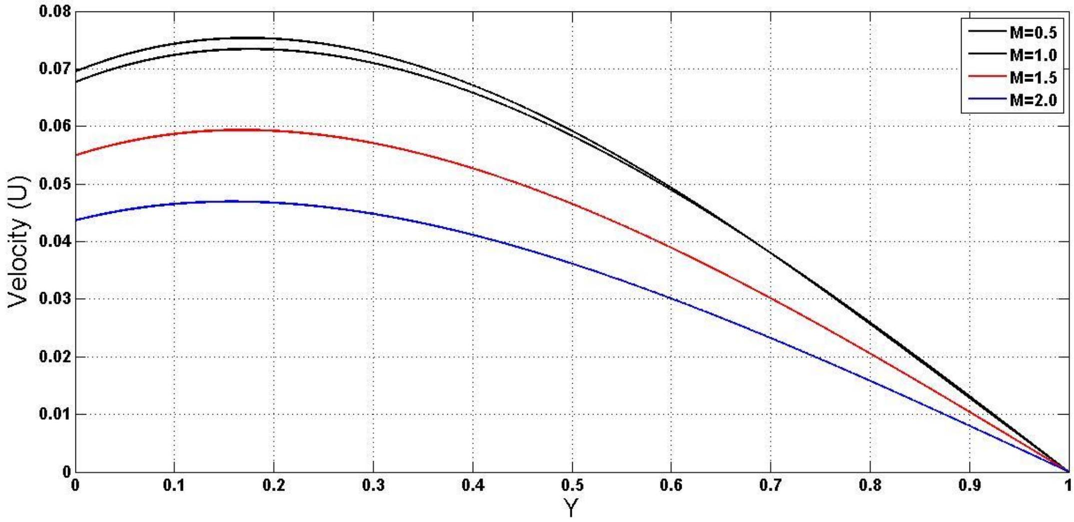


**Figure 7: Deviation of velocity for MHD for constants values of (λ = γ = 1, Br=0.001, Da=0.1)**

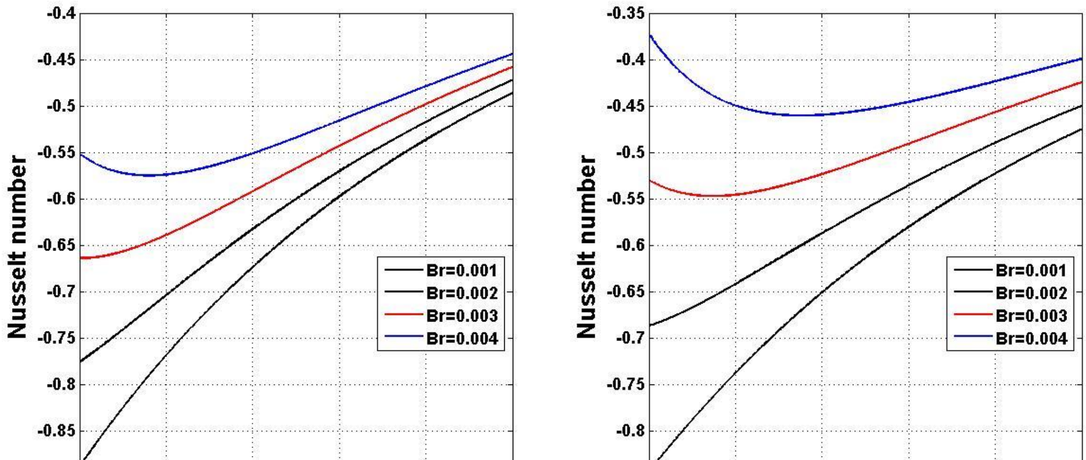


**Figure 8: Variation for Nusselt number for Br at (a) y =0 and (b) y=1 for constants values of (λ = γ = 1, M=0.5, Da=0.1)**

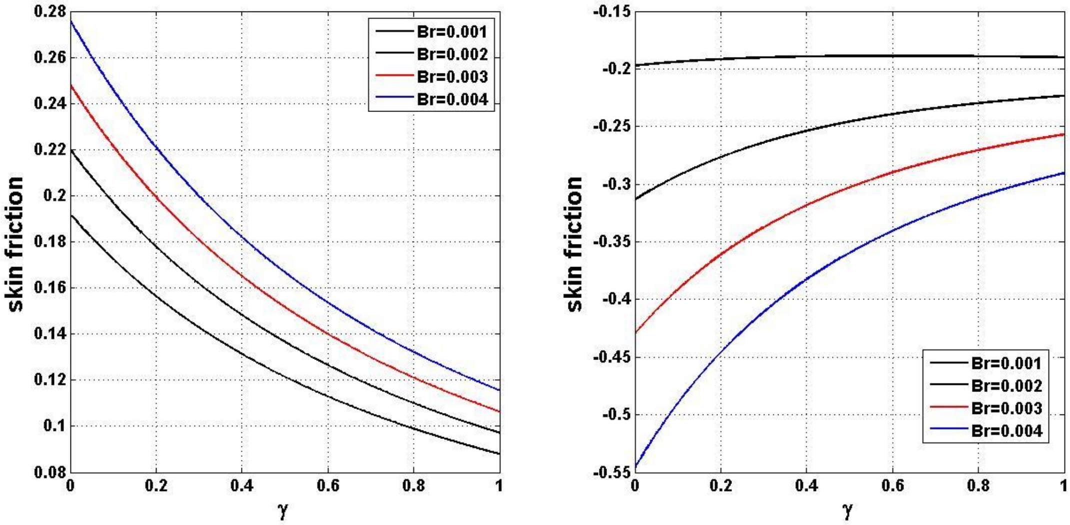


**Figure 9: Variation for skin friction for Br at (a) y =0 and (b) y=1 for constants values of (λ = γ = 1, M=0.5, Da=0.1)**

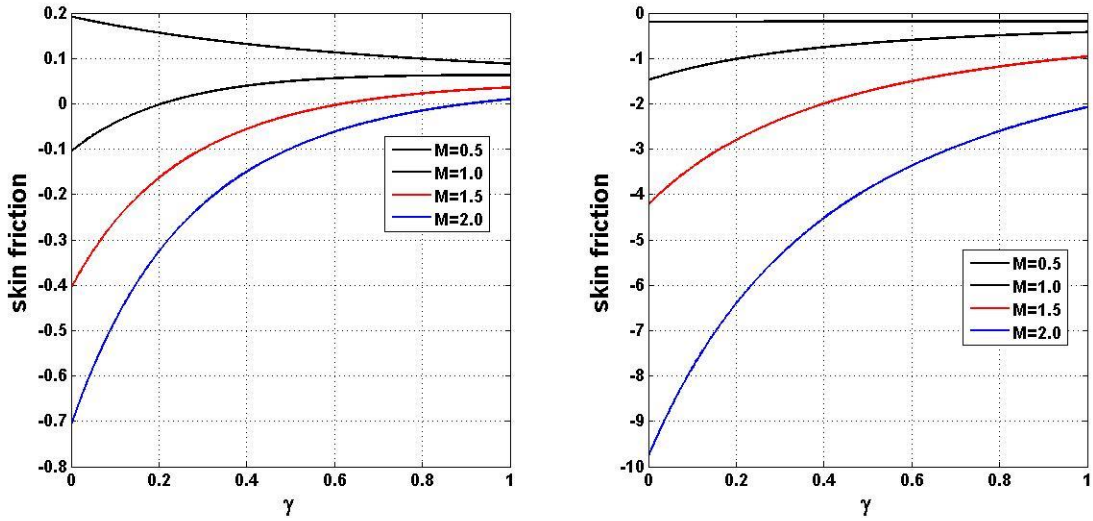


**Figure 10: Variation for skin friction for M at (a) y =0 and (b) y=1 for constants values of (λ = γ = 1, Br=0.001, Da=0.1)**

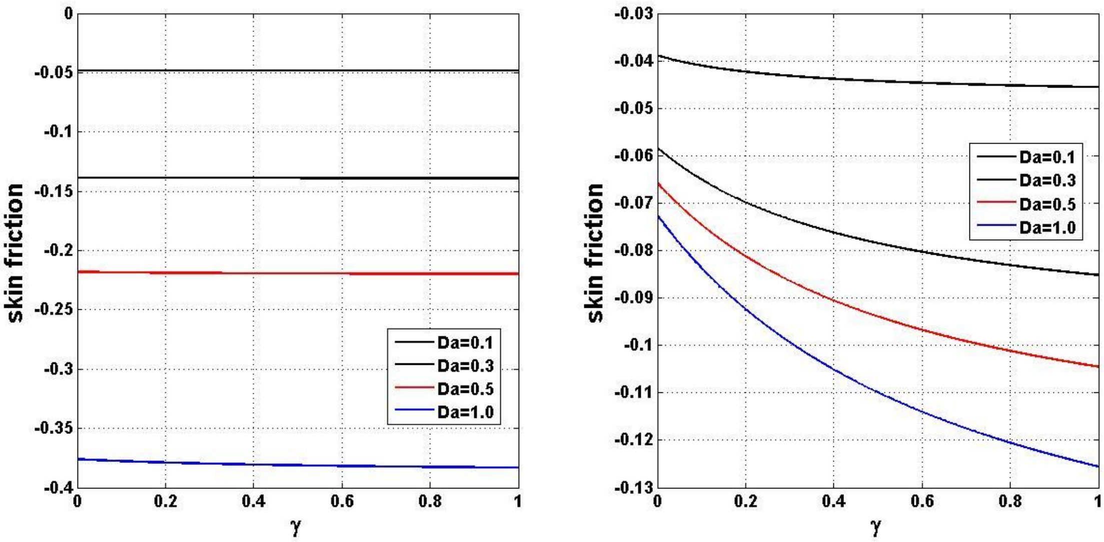


**Figure 11: Variation for skin friction for Da at (a) y =0 and (b) y=1 for constants values of (λ = γ = 1, M=0.5, Br=0.001)**

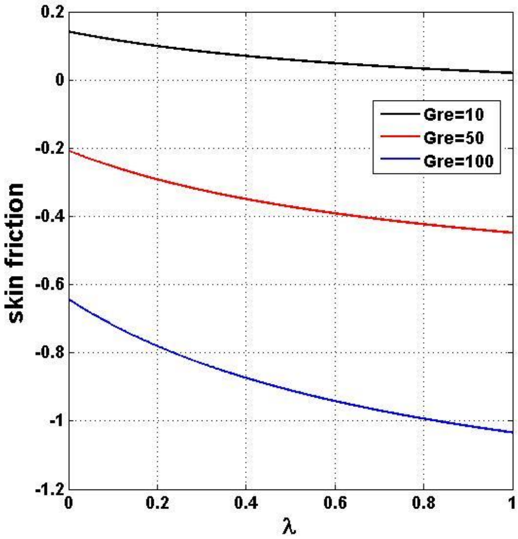


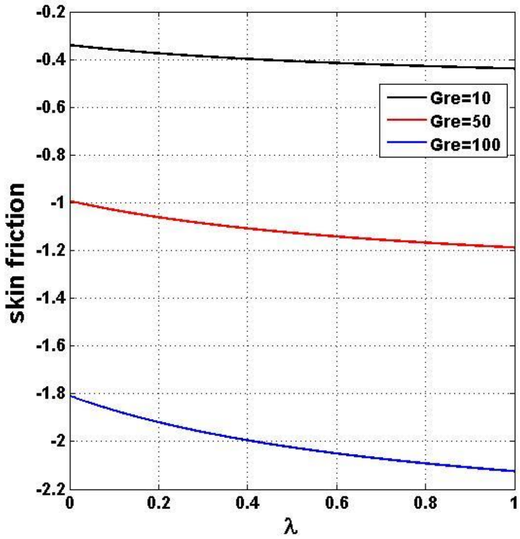


**Figure 12: Variation for skin friction for Gre at (a) y =0 and (b) y=1 for constants values of (λ = γ = 1, M=0.5, Br=0.001)**

**Table 1: Computations of comparison between the work of Jha and Gwandu [1] with the current analysis for temperature and velocity distributions for λ = γ = 1, M = 0.5 when Gre=1, Br and A is zero respectively and Da = 1000.**

| Y | Jha and Gwandu [1] θ (Y) U(Y) | | Present work θ(Y) U(Y) | |
|---|---|---|---|---|
| 0.1 | 0.4500 | 0.0843 | 0.4500 | 0.0843 |
| 0.2 | 0.4000 | 0.0856 | 0.4000 | 0.0856 |
| 0.3 | 0.3500 | 0.0831 | 0.3500 | 0.0831 |
| 0.4 | 0.3000 | 0.0772 | 0.3000 | 0.0772 |
| 0.5 | 0.2500 | 0.0686 | 0.2500 | 0.0686 |

## 6. CONCLUSION

The present study analyzes the consequences of porosity parameter and viscous dissipation on the steady MHD mixed convection flow of a viscous, electrically conducting fluid traveling vertically across an isothermally heated parallel plate micro-channel embedded with porous medium, with one surface exhibiting super-hydrophobic slip and temperature jump and the other did not. Semi-analytical method (perturbation series approach) was employed to generate the steady state solutions for temperature, velocity, rate of heat transfers and sheer stress. The influence of pertinent parameter dictating the flow configuration is discussed in detail using various plots. Viscous dissipation and Darcy porous effects are very vital in most lubrication industries. This study can therefore find relevance in science, engineering, and industrial technologies such as cooling of electrical appliances, geothermal energy, porous solids drying, thermal insulation, gas drainage, plasma physics, gas turbines, fossil fuel combustion, food processing industries, to mention a few.

The following is an overview of the significant findings from this study:

i. The maximum velocity attained by heating the super-hydrophobic surface is smaller than that recorded by heating the no-slip surface when there is a temperature jump and no super-hydrophobic slip or both. The opposite is true if there is a super-hydrophobic slide but no temperature surge. When neither exists, the maximum velocities are equal.

ii. As the Brinkman number parameter goes up, the velocity of the fluid and the heat gradient grows noticeably, but the local skin friction goes down at y = 0 and up at y = 1.

iii. Upon increasing the Darcy permeability parameter, drag forces diminish; hence the fluid mobility in the micro-channel significantly improve. Also, the sheer stress at both micro-channel walls exhibits comparable trends with the same consequence

iv. Mixed convection parameter is seen to significantly accelerate the fluid flow in the microchannel

v. Velocity gradient peters out upon raising the levels of magnetic parameter due to the Lorentz forces which manifest under the MHD effect.

vi. By uplifting the values of Br, the heat transfer rate is encouraged at the no-slip plate, whereas at the super-hydrophobic surface, the trend is the opposite.

vii. At the both microchannel walls, the skin friction exhibit similar retarding effects for growing values of Gre.

**Competing Interests**

The authors declare no competing interests.

## REFERENCES


1. Jha, B. K., & Gwandu, B. J. (2018). MHD free convection flow in a vertical slit micro-channel with super-hydrophobic slip and temperature jump: Heating by constant wall temperature. *Alexandria engineering journal*, *57*(4), 2541-2549.
2. Jha, B. K., Aina, B., & Ajiya, A. T. (2015). MHD natural convection flow in a vertical parallel plate microchannel. *Ain Shams Engineering Journal*, *6*(1), 289-295.
3. Hamza, M. M., Ojemeri, G., & Ahmad, S. K. K. (2023). Theoretical study of ARRHENIUS-controlled heat transfer flow on natural convection affected by an induced magnetic field in a micro-channel. *Engineering Reports*, e12642.
4. Ojemeri, G., & Hamza, M. M. (2022). Heat transfer analysis of Arrhenius-controlled free convective hydromagnetic flow with heat generation/absorption effect in a micro-channel. *Alexandria Engineering Journal*, *61*(12), 12797-12811.
5. Jha, B. K., & Malgwi, P. B. (2019). Hall current and ion-slip effects on free convection flow in a vertical microchannel with an induced magnetic field. *Heat Transfer—Asian Research*, *48*(8), 3812-3830.
6. Jha, B. K., & Aina, B. (2016). Role of induced magnetic field on MHD natural convection flow in vertical microchannel formed by two electrically non-conducting infinite vertical parallel plates. *Alexandria Engineering Journal*, *55*(3), 2087-2097.
7. Jha, B. K., Malgwi, P. B., & Aina, B. (2018). Hall effects on MHD natural convection flow in a vertical microchannel. *Alexandria Engineering Journal*, *57*(2), 983-993.
8. Chen, C. O. K., & Weng, H. C. (2005). Natural convection in a vertical microchannel.
9. Jha, B. K., & Aina, B. (2015). Mathematical modelling and exact solution of steady fully developed mixed convection flow in a vertical micro-porous-annulus. *Afrika Matematika*, *26*, 1199-1213.
10. Buonomo, B., & Manca, O. (2012). Transient natural convection in a vertical microchannel heated at uniform heat flux. *International Journal of Thermal Sciences*, *56*, 35-47.
11. Weng, H. C. (2009). Drag reduction and heat transfer enhancement over a heated wall of a vertical annular microchannel. *International journal of heat and mass transfer*, *52*(3-4), 1075-1079.
12. Jha, B. K., Aina, B., & Isa, S. (2015). Fully developed MHD natural convection flow in a vertical annular microchannel: an exact solution. *Journal of King Saud University-Science*, *27*(3), 253-259.
13. Jha, B. K., Aina, B., & Isa, S. (2015). Fully developed MHD natural convection flow in a vertical annular microchannel: an exact solution. *Journal of King Saud University-Science*, *27*(3), 253-259.
14. Ojemeri, O., Omokhuale, E., Hamza, M., Onwubuya, I., & Shuaibu, A. (2023). A Computational Analysis on Steady MHD Casson Fluid Flow Across A Vertical Porous Channel Affected By Thermal Radiation Effect. *International Journal of Science for Global Sustainability*, *9*(1), 13-13.
15. Hamza, M. M. (2018). Free convection slip flow of an exothermic fluid in a convectively heated vertical channel. *Ain shams Engineering journal*, *9*(4), 1313-1323.
16. Taid, B. K., & Ahmed, N. (2022). MHD free convection flow across an inclined porous plate in the presence of heat source, Soret effect, and chemical reaction affected by viscous dissipation Ohmic heating. *Biointerface Research in Applied Chemistry*, *12*(5), 6280-6296.
17. Osman, H. I., Omar, N. F. M., Vieru, D., & Ismail, Z. (2022). A Study of MHD Free Convection Flow Past an Infinite Inclined Plate. *Journal of Advanced Research in Fluid Mechanics and Thermal Sciences*, *92*(1), 18-27.
18. Siva, T., Jangili, S., & Kumbhakar, B. (2021). Heat transfer analysis of MHD and electroosmotic flow of non-Newtonian fluid in a rotating microfluidic channel: an exact solution. *Applied Mathematics and Mechanics*, *42*(7), 1047-1062.
19. Choudhury, S., & Dey, D. HEAT AND MASS TRANSFER FOR VISCO-ELASTIC MHD BOUNDARY LAYER FLOW PAST A VERTICAL PERMEABLE PLATE.
20. Sandeep, N., & Sugunamma, V. (2013). Effect of inclined magneticfield on unsteady free convection flow of a dusty viscous fluid between two infinite flat plates filled by porous medium. *International Journal of Applied Mathematics and Modeling*, *1*(1), 16-33.
21. Manyonge, W. A., Kiema, D. W., & Iyaya, C. C. W. (2012). Steady MHD poiseuille flow between two infinite parallel porous plates in an inclined magnetic field.
22. Geethan Kumar, S., Kiran Kumar, R. V. M. S. S., Vinod Kumar, G., & Varma, S. V. K. (2016). Soret and radiation effects on MHD free convection slip flow over an inclined porous plate with heat and

mass flux. *Advanced science, engineering and medicine*, *8*(12), 986-995.

23. Sivaiah, G., & Reddy, K. J. (2017). Unsteady MHD heat and mass transfer flow of a radiating fluid past an accelerated inclined porous plate with Hall current. *International Journal of Research-Granthaalayah*, *5*(7), 42-59.
24. Jha, B. K., & Gwandu, B. J. (2019). MHD free convection in a vertical slit micro-channel with super-hydrophobic slip and temperature jump: non-linear Boussinesq approximation approach. *SN Applied Sciences*, *1*, 1-10.
25. Jha, B. K., & Gwandu, B. J. (2021). MHD free convection flow in a vertical porous super-hydrophobic micro-channel. *Proceedings of the Institution of Mechanical Engineers, Part E: Journal of Process Mechanical Engineering*, *235*(2), 470-478.
26. Ramanuja, M., Krishna, G. G., Sree, H. K., & Radhika, V. N. (2020). Free convection in a vertical slit micro-channel with super-hydrophobic slip and temperature jump conditions. *Int. J. Heat Technol*, *38*(3), 738-744.
27. Hatte, S., & Pitchumani, R. (2021). Analysis of convection heat transfer on multiscale rough superhydrophobic and liquid infused surfaces. *Chemical Engineering Journal*, *424*, 130256.
28. Makinde, O. D., & Aziz, A. (2011). Boundary layer flow of a nanofluid past a stretching sheet with a convective boundary condition. *International Journal of Thermal Sciences*, *50*(7), 1326-1332.

**Nomenclature**

$B_0$ =constant magnetic flux density [kg/s$^2$.m$^2$]
g=gravitational acceleration [m/s$^2$]
h= wideness of the channel [m]
$C_p C_v$=specific heats at constant pressure and constant volume [Jkg$^{-1}$K$^{-1}$]
$\lambda$ =dimensionless slip length parameter
$\gamma$ =dimensionless temperature jump parameter
M= magnetic field
Br=Brinkman number
Da=Darcy number
$\frac{Gr}{Re} = Gre$ = Mixed convection parameter
$\frac{dP}{dX} = A$ = Pressure gradient
Nu=dimensionless heat transfer rate
T=dimensionless temperature of the fluid [K]
$T_0$=reference temperature [K]
u=dimensionless velocity of the fluid [ms$^{-1}$]
y= dimensionless distance between plates
$U_0$=reference velocity [ms$^{-1}$]

**Greek letters**

$\beta$ =thermal expansion coefficient [K$^{-1}$]
$\beta_t \beta_v$ =dimensionless variables
$\mu$ =variable fluid viscosity [kgm$^{-1}$s$^{-1}$]
k=thermal conductivity [m.kg/s$^3$.K]
$\alpha$ =thermal diffusivity [m$^2$s$^{-1}$]
$\gamma_s$ = ratios of specific heats ($C_p C_v$)
$\sigma$ =electrical conductivity of the fluid [s$^3$m$^2$/kg]
$\rho$ = density of the fluid [kgm$^{-3}$]
$\nu$ =fluid kinematic viscosity [m$^2$s$^{-1}$]

**Appendix**

$$V_1 = \frac{1}{1+\gamma}, V_2 = \frac{-1}{1+\gamma}, V_3 = \frac{\lambda V_5 - V_6 - V_4 a_2}{a_1}, V_4 = \frac{V_5 a_4 + V_6 a_5}{a_3}, V_5 = \frac{GreV_1}{R}, V_6 = \frac{GreV_2}{R} + A, V_7 = \frac{a_5 - a_8 - a_7\gamma}{1+\gamma}$$

$$V_3 = \gamma(a_8 + V_7) - a_5, F_1 = \frac{\lambda F_{11} - F_{10} - F_2 a_2}{a_1}, F_2 = \frac{F_{14}}{F_{13}}, F_3 = \frac{k_1}{3R}, F_4 = \frac{k_2}{2\sqrt{R}}, F_5 = \frac{-k_3}{2\sqrt{R}}$$

$$F_6 = \frac{k_4}{3R}, F_7 = \frac{-k_5}{R}, F_8 = \frac{V_7}{R}, F_9 = \frac{V_8 + 2F_7}{R}, F_{10} = F_3 + F_6 + F_9, F_{11} = 2F_3\sqrt{R} + F_4 + F_5 - 2F_6\sqrt{R} + F_8, F_{12} = 2F_4 e^{2\sqrt{R}} + F_4 e^{\sqrt{R}} + F_5 e^{-\sqrt{R}} + 2F_6 e^{-2\sqrt{R}} + F_7 + F_8 + F_9, F_{13} = a_1 e^{-\sqrt{R}} - a_2 e^{\sqrt{R}}$$

$$F_{14} = F_{10} e^{\sqrt{R}} - \lambda F_{11} e^{\sqrt{R}} - a_1 F_{12}, a_1 = 1 - \lambda\sqrt{R}, a_2 = 1 + \lambda\sqrt{R}, a_3 = a_1 e^{-\sqrt{R}} - a_2 e^{\sqrt{R}}$$

$$a_4 = -a_1 - \lambda e^{\sqrt{R}}, a_5 = e^{\sqrt{R}} - a_1, k_1 = \frac{a_1}{4R}, k_2 = \frac{a_2}{R}, k_3 = \frac{a_3}{R}, k_4 = \frac{a_4}{4R}, k_5 = \frac{a_5}{2}, R = M^2 + \frac{1}{Da}$$